



**HAL**  
open science

## Multi-scale Curvature Analysis and Correlations with the Fatigue Limit on Steel Surfaces after Milling

Margot Vulliez, Matthew Gleason, Aurélien Souto-Lebel, Yann Quinsat, Claire Lartigue, Steven Kordel, Adam Lemoine, Christopher Brown

► **To cite this version:**

Margot Vulliez, Matthew Gleason, Aurélien Souto-Lebel, Yann Quinsat, Claire Lartigue, et al.. Multi-scale Curvature Analysis and Correlations with the Fatigue Limit on Steel Surfaces after Milling. 2nd CIRP Conference on Surface Integrity (CSI), May 2014, Birmingham, United Kingdom. pp.308-313, 10.1016/j.procir.2014.04.052 . hal-01010455

**HAL Id: hal-01010455**

**<https://hal.science/hal-01010455>**

Submitted on 8 Dec 2014

**HAL** is a multi-disciplinary open access archive for the deposit and dissemination of scientific research documents, whether they are published or not. The documents may come from teaching and research institutions in France or abroad, or from public or private research centers.

L'archive ouverte pluridisciplinaire **HAL**, est destinée au dépôt et à la diffusion de documents scientifiques de niveau recherche, publiés ou non, émanant des établissements d'enseignement et de recherche français ou étrangers, des laboratoires publics ou privés.

# Multi-scale curvature analysis and correlations with the fatigue limit on steel surfaces after milling

Margot Vulliez<sup>a</sup>, Matthew A. Gleason<sup>b</sup>, Aurélien Souto-Lebel<sup>a</sup>, Yann Quinsat<sup>a</sup>, Claire Lartigue<sup>a</sup>, Steven P. Kordell<sup>b</sup>, Adam C. Lemoine<sup>b</sup>, Christopher A. Brown<sup>b\*</sup>

<sup>a</sup>LURPA, (ENS Cachan, Université Paris-sud 11)  
61 Av. du Pdt Wilson, 94230 Cachan, France

<sup>b</sup>Surface Metrology Laboratory, Worcester Polytechnic Institute, Worcester, Massachusetts 01609 USA

\* Corresponding author. Tel.: +1-508-831-5627; fax: +1-508-831-5673. E-mail address: brown@wpi.edu.

---

## Abstract

A strong correlation ( $R^2 > 0.96$ ) is found between machined surfaces and their fatigue limits. In a larger study, the four-point bending fatigue limit was determined on steel specimens milled with two different conditions, in two directions, with and without residual stresses relieved. Curvature analysis is shown here, based on Heron's formula, as a function of scale and position, on profiles extracted parallel to the direction of maximum tensile stress, from areal texture measurements. Several combinations of parameters are regressed linearly with the fatigue limits over a range of scales. The strongest correlations are found with the mean curvature plus two standard deviations, at a scale of  $610\mu\text{m}$ . The correlation varies smoothly, although not monotonously, with respect to decreasing scale, with  $R^2$  falling to zero at  $100\mu\text{m}$ .

*Keywords: roughness; fatigue; machining*

---

## 1. Introduction

The objective of this work is to investigate the strength of correlations between the curvatures of the topographies of ball-end milled steel specimens and the fatigue limits in four-point bending. Curvatures are calculated from profiles extracted from measured topographies. The curvatures change with position and with the scale of observation and provide an indication of the integrity of the surface topography.

A quantitative understanding of the relation between the topography and the fatigue limit can facilitate better product and process design for parts where fatigue resistance is important. The discovery of strong correlations between topographic characterization parameters and the fatigue limit could depend on identifying the appropriate characterization parameter and the appropriate scale, which would be similar to correlations that have been found with adhesion, friction, fracture surfaces, and mass transfer [1-5].

### 1.1. State-of-the-art

Although it is generally accepted that topography influences the fatigue limit, quantitative descriptions with experimental confirmation appear to be rare. Geometric stress concentration ( $K_t$ ) is based on curvature ( $k=1/\rho$ ) and the depth of a notch ( $t$ ) [6]:

$$K_t = 1 + 2 (t/\rho)^{1/2} \quad (1)$$

Models have been proposed that use conventional roughness characterizations in the calculation of stress concentrations. Arola and Ramulu [7] studied rough surface topographies of machined fiber reinforced composites. They replaced notch depth with the conventional roughness characterization parameters:  $R_a$  average roughness,  $R_t$

maximum peak to valley depth,  $R_z$  average of the greatest peak to valley depth in five sections. This produces an expression for tensile loading:

$$K_t = 1 + 2 (R_a/\rho)(R_t/R_z) \quad (2)$$

For machined metals, however, the surface roughness parameters appear not to be sufficient, at least on an individual basis, for estimating fatigue strength [8]. Cracks that lead to fatigue failure of mechanical parts have been found to originate from micro-scratches on the surface, which are not described by conventional roughness parameters [9]. Cracks are not restricted to originating on topographic features and could originate on microstructural elements.

Useful expressions for the stress concentrations could depend on the material and the preparation of the surface. The dependence of the stress concentration on the curvatures calculated from measured topographies seems like a logical extension of the fundamental development of stress concentrations for notches. There are established procedures for strength analysis in shafts and axles that are based on the static strength with stress concentration factors (e.g., DIN 743 [10]).

The roughness of topographies that results from machining of metals has regular and irregular, or chaotic, components [11,12]. Machined surfaces also have regular components at larger scales, which are usually associated with the feed. The irregular components have been modeled as stochastic, successfully reproducing Abbot curves [13]. These irregular topographies contain features with a range of curvatures that vary with scale and position. These features defy any simple curvature descriptions as smooth notches.

Recently, methods of calculating curvatures of roughness profiles on a multi-scale basis have been proposed [14,15]. The current work applies these recent developments of the multi-scale calculation of curvatures on profiles to the characterization of milled surfaces, and then uses it for correlation with the fatigue limit.

A strong correlation is being sought here between some representation of the curvature of features on the surface and the fatigue limit in four point bending. The fatigue specimens are all machined with a ball-nose endmill, the same feed per tooth but with different tool inclinations, and different feed directions. Because the influence of residual stress and micro-geometry can be coupled, in four specimens the residual stresses were removed, leaving only the influence of the micro-geometry. The curvature is calculated as a function of scale and position. It is not immediately obvious how to use this myriad of calculated curvatures to find a strong correlation with the fatigue limit. Several statistical representations of curvature are investigated. A method is proposed for finding the appropriate scale for calculating the curvature (patent pending).

$\rho$	radius (reciprocal of curvature, k)
k	curvature varying with scale and position
R	linear regression coefficient
$\mu()$	mean of the indicated value
$\sigma()$	standard deviation of the indicated value

## 2. Methods

Bainitic 50CrMo4 steel ( $R_e=480$  Mpa;  $R_m=1080$  Mpa) was machined by ball-end milling on a Mikron UCP710 five-axis vertical machining centre to create six different types of surfaces on approximately 80 specimens for fatigue testing. These specimens have been studied extensively previously [9,11,12,16,17]. The tool inclination relative to the surface is defined by the lead angle  $\beta$ , as shown in Fig. 1. Two values of  $\beta$  were studied ( $\beta = 45^\circ$  and  $\beta = -3^\circ$ ). The specimen dimensions are 100x20x4mm. The machining conditions are listed in Table 1. Four of the machined specimens were subjected to a stress-relieving heat treatment at 470°C for one hour, with a cooling rate of 90°C/hr.

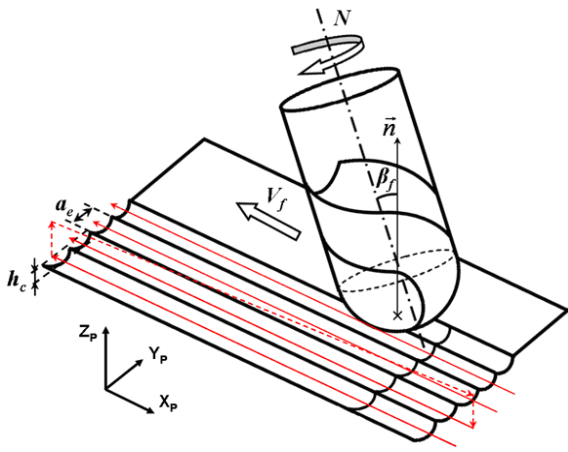


Fig. 1. Schematic of ball-end milling with an inclined tool indicating only a regular component of the machined surface topography

Table 1. Machining conditions

Spindle speed	$\omega$	9550 rpm
Feed per tooth	$f$	400 $\mu\text{m}$ per tooth
Depth of cut	$p$	500 $\mu\text{m}$
Step over	$a_e$	450 $\mu\text{m}$
Tool nose radius	$r$	5mm
Inclination angles	$\beta_f$	45°, -3°

As indicated below in Table 2 during the machining the milling tool was fed both transversely and longitudinally with respect to the eventual loading direction, i.e., tensile stress axis, in four-point bending fatigue tests [17]. Each of the two inclinations was repeated in both directions for a total of four specimens. These four specimens were subjected to the stress relieving heat treatment. Two additional specimens were machined in the transverse direction and were not subjected to the heat treatment.

The nominal scallop height,  $h_c$ , can be calculated to be 5 $\mu\text{m}$  from the step over and the tool nose radius by theoretical approximation ( $h_c = a_e^2/8r$ ). This expression is based on smooth surface generation by a smooth tool edge with no ploughing.

The machined surfaces were measured with a 3D Stil Microstation. This is a horizontal profile-scanning instrument with a confocal chromatic height sensor with a 100 $\mu\text{m}$  vertical range. All measurements were cropped to 700x700 $\mu\text{m}$ . A modal outlier filter [18] was used to eliminate spike artefacts from the measurements. This modal filtering is characterized by two parameters: the risk ( $\alpha=10^{-5}$  here) and the number of modes for the calculation (250 here). Thresholding and Gaussian filtering were attempted but not used. According to area-scale analysis [19,20], these filters did not work as well as the modal filter for removing spike-like measurement artifacts. The relative areas were higher for these methods. In the final analysis, only the modal filtering was used.

Curvature calculations were done on a total of 1120 profiles extracted parallel to the axis of maximum tensile stress. Because the sampling intervals in the profiling direction were different for two of the measurements, 0.625 $\mu\text{m}$  versus 0.5 $\mu\text{m}$ , the common interval of 0.625 $\mu\text{m}$  was chosen and the profiles closest to that sampling interval were extracted.

A geometric method, based on Heron's formula [14, 15], is used to calculate the curvatures based on three heights equally separated laterally. The lateral spacing of the two exterior heights is used to represent the scale. For the calculation of the curvature from three measured heights, the algorithm steps along a profile of height sample by height sample, calculating the curvature as a function of position at one scale, and then the calculation repeats for each scale.

A strict protocol was followed for the fatigue tests, which were done in four-point bending [17]. The two extreme loading points (or, more precisely, loading lines) were 50mm apart, and the central, interior loading points were 20mm apart.

### 3. Results

The fatigue results are shown in Table 2, along with the machining conditions and an indication of whether or not they were stress relieved. The specimens with polished surfaces have a fatigue limit of 755MPa [17].

Examples of renderings of measured surfaces are shown in Figures 2 a&b, from specimens milled with inclination of  $-3^\circ$  and  $45^\circ$  with the stress relieved. The fine-scale roughness, which could be described as variations from an otherwise smooth surface that is defined only by the tool shape and motion, is clearly evident, appearing as irregular or chaotic topographic elements.

Table 2. Fatigue limits, machining conditions, and stress relief

stress relieved	Angles $\beta_f$ deg	Feed direction	Fatigue limit MPa
no	-3	transverse	670
yes	-3	transverse	633
yes	45	transverse	675
no	45	transverse	680
yes	-3	longitudinal	735
yes	45	longitudinal	715

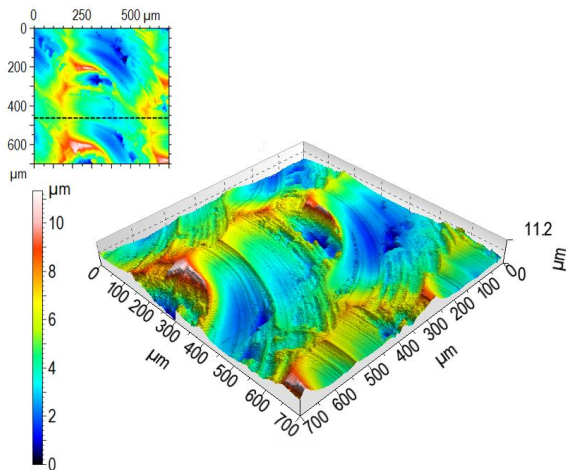


Fig. 2a. Rendering of a measurement of the surface milled with an inclination of  $-3^\circ$  and then stress relieved and subjected to transverse loading as indicated by the line in the upper left image.

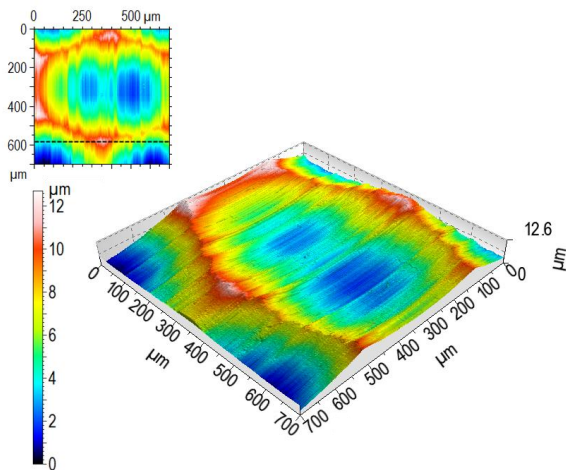


Fig. 2b. Rendering of a measurement of the surface milled with an inclination of  $45^\circ$  and then stress relieved and subjected to longitudinal loading, as indicated by the line in the upper left image.

The roughness values for the height parameters are shown in Table 3. The S parameters are means and standard deviations of the areal measurements. It is noted that the identical machining conditions do not produce surfaces with identical roughness parameters. The peak-to-valley roughness values ( $S_t$ ) differ clearly from the theoretical calculation of the cusp height ( $h_c=5\mu\text{m}$ ) in all cases.

Table 3. Conventional roughness characterizations of means of heights. All values are in micrometres.

Specimen*	Sa	Sq	St	Sv
N-3T	1.39	1.79	11.2	3.81
Y-3T	1.45	1.73	17.2	5.71
Y45T	1.59	1.92	11.8	6.35
N45T	1.46	1.76	10.3	5.29
Y-3L	1.72	2.05	13.8	6.66
Y45L	2.28	2.71	20.48	7.99

\*Stress relief Y/N, angle, direction

Figures 3a&b show profiles, and curvatures versus position at scales of 150 and 500µm. The positive curvatures are concave up and tend to be at the bottoms of valleys, more likely for fatigue crack initiation.

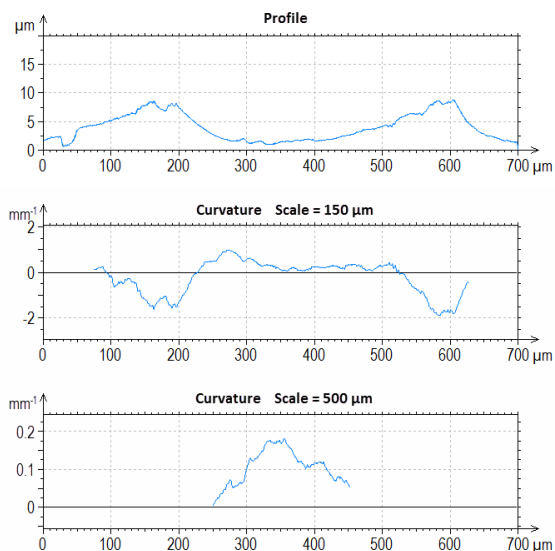


Fig. 3a. Profile, extracted as indicated in Fig. 2a, with corresponding curvatures versus position at scales of 150 and 500µm.

Figures 4&5 show the curvatures versus position and scale. Curvature is plotted on the vertical axis and is also represented by colour. The horizontal axes denote the positions along the extracted profile and the scale at which the curvature is calculated. As the scale increases, there are fewer positions at which the curvature can be calculated, and the plot along the profile axis becomes narrower.

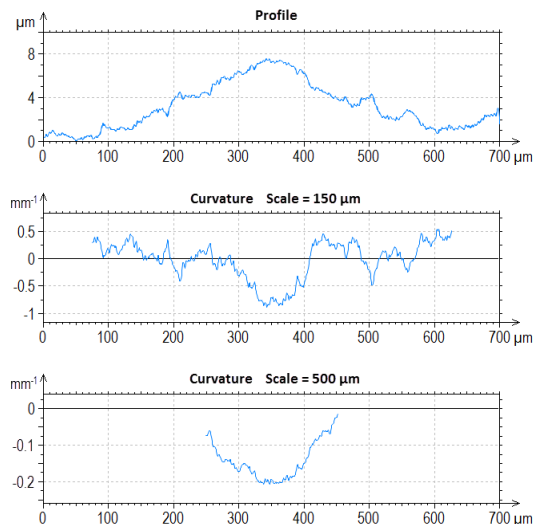


Fig. 3b. Profile, extracted as indicated in Fig. 2b, with corresponding curvatures versus position at scales of 150 and 500µm.

At the larger scales, the values of the curvatures diminish and tend towards zero, consistent with the flat nature of the specimens at larger scales. Figures 4a&b go up to a scale of 600 $\mu\text{m}$ , where it is difficult to discern any change in curvature with position in contrast to the finer scales. At the finest scales changes in curvature with position are obvious. Therefore, additional plots are shown at the larger scales with the curvature axis re-scaled in order to make the changes in curvature with position along the profile more obvious.

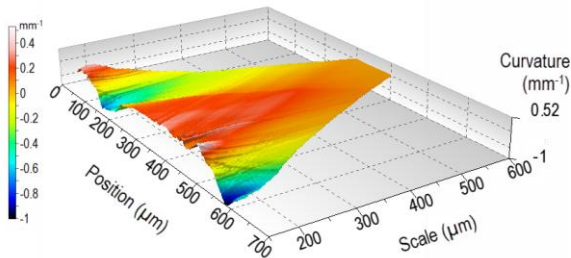


Fig. 4a. Profile curvatures (vertical axis, colour) as a function of scale and position from the surface shown in Figures 2a and 3a milled at  $-3^\circ$ .

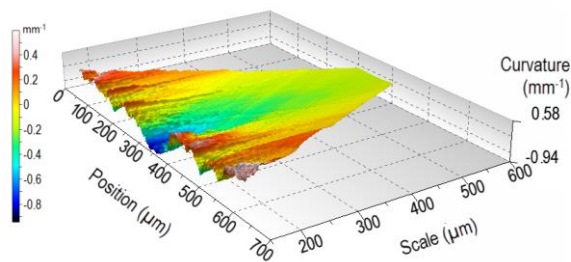


Fig. 4b. Profile curvatures (vertical axis, colour) as a function of scale and position from the surface shown in Figures 2b and 3b milled at  $45^\circ$ .

Figures 5a&b show the curvatures versus position at the largest scales.

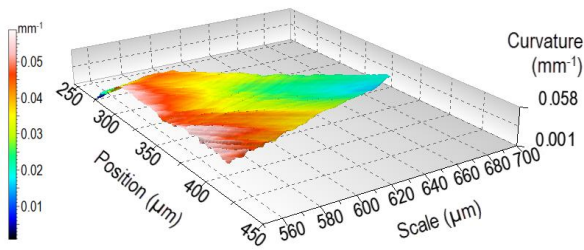


Fig. 5a. Profile curvatures (vertical axis, colour) as a function of scale and position from the surface shown in Figures 2a and 3a milled at  $-3^\circ$ .

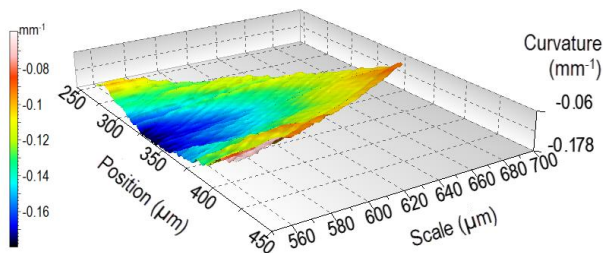


Fig. 5b. Profile curvatures (vertical axis, colour) as a function of scale and position from the surface shown in Figures 2b and 3b milled at  $45^\circ$ .

Several criteria, combinations of the curvature and roughness parameters, were regressed linearly with the fatigue limit over a range of scales. The most successful criteria, shown in Table 4, come from analyses of the distribution of the curvatures. The mean and standard deviations of the curvatures are calculated on each profile at each scale. The

maximum values from these calculations from all of the 1120 profiles might match the most dangerous feature on the surface for initiating a fatigue crack. Regression analyses with the fatigue limit versus these maximum values are performed over all the scales in the measurements. The results are shown in Table 4 with the regression coefficients and scales.

Table 4. Regression coefficients for several candidate criteria

Method	max R <sup>2</sup>	scale (μm)
$max(k)$	0.76	620
$\underline{\mu} (10 max(k))$	0.8	618
$max(\mu(k) + \sigma(k))$	0.65	620
$max(\mu(k) + 2\sigma(k))$	0.96	610

Fig. 6 shows a plot of the regression coefficient R<sup>2</sup> as a function of scale for the most successful criterion, maximum mean of the curvatures plus two standard deviations ( $max(\mu(k) + 2\sigma(k))$ ). The maximum R<sup>2</sup> (0.96) is reached at a scale of 610μm. Fig. 7 shows the plot of  $max(\mu(k) + 2\sigma(k))$  versus the fatigue limit at 610μm. This remarkably strong correlation is found only at a scale of 610μm.

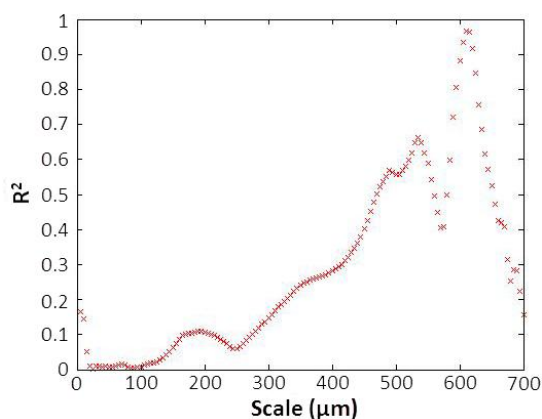


Fig. 6. The coefficient of linear regression curvature (mean of the curvatures, plus two standard deviations) regressed with the fatigue limit, plotted versus scale.

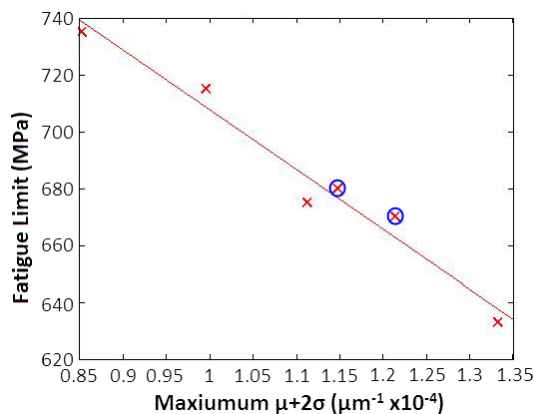


Fig. 7. Mean of the curvatures, plus two standard deviations versus the fatigue limit at a scale of 610μm. The two circled results were from specimens that were not heat treated.

#### 4. Discussion

The curvature calculated from measured profiles provides an indication of the stress concentration that would influence fatigue strength. Curvature, or radius, of notch roots has been used in the traditional, theoretical developments of the calculation of stress concentrations.

Fatigue cracks can initiate on things other than topographic features. However, in this study, it has been decided to focus on the machining and resulting topography. However, the strong correlation of the fatigue limit with the curvature confirms our choice, regardless of the heat treatment and the direction of machining relative to the applied tensile stress.

This work suggests that a systematic approach to finding the relations between roughness and fatigue limit could be based on determining the scale at which the mean curvature correlates most strongly with the fatigue limit.

The scale at which the strongest correlation is found is larger than the feed per tooth. It would be interesting to see if the maximum  $R^2$  would also be found at this same scale if the machining were to be performed with finer feeds per tooth.

The negative curvatures (convex up) should not be expected to influence the fatigue limit. At the scale of the strongest correlation it is noted that there is little negative curvature. In any event the consideration of the mean plus two standard deviations of the curvatures at each scale is robust with respect to the inclusion of negative curvatures. This approach guarantees that the features that are the most likely to provide dangerous stress concentrations will be considered.

The stress-relieving heat treatment seems to have little influence on the correlation. As indicated in Fig. 5 the two specimens without stress relief appear to be on the same curve as those with stress relief. In situations where residual stresses play a larger role, the influence of the residual stress on the fatigue limit might be considered by a superposition of the residual stress on the applied stresses. Then the same sort of calculation of curvature could be used to determine the influence of the microgeometry.

## 5. Conclusions

- The maximum mean curvature plus two standard deviations correlates strongly with the limit in fatigue at a scale of 610 $\mu$ m of the ball-end milled steel parts in this study.
- The strength of the correlations with the multi-scale curvature parameters and the fatigue limit varies with the scale of calculation.
- A method has been developed and demonstrated for determining for finding the appropriate scale for multi-scale parameters for predicting fatigue behaviour when applied to certain material and manufacturing process.

## Acknowledgements

The authors gratefully acknowledge the steel manufacturer ASCOMETAL, for providing the steel and performing fatigue tests; DigitalSurf for generously providing MountainsMap software for calculating conventional roughness characterization parameters and rendering images. Sfrax was used for area-scale calculations and was provided by Surftract, which is owned by co-author Brown. A provisional patent has been filed in the United States on this method for determining the fatigue limit from the surface topography.

## References

1. Brown, C.A., Siegmans, S., 2001. Fundamental scales of adhesion and area-scale fractal analysis, *International Journal of Machine Tools and Manufacture* 41, p. 1927.
2. Berglund, J., Brown, C.A., Rosen, B.-G., Bay, N., 2010. Milled Die Steel Surface Roughness Correlation with Steel Sheet Friction, *CIRP Annals Manufacturing Technology* 59, p. 577.
3. Berglund, J., Agunwamba, C., Powers, B., Brown, C.A., Rosén, B.-G., 2010. On Discovering Relevant Scales in Surface Roughness Measurement- An Evaluation of a Band-Pass Method, *Scanning* 32, p. 244.
4. Cantor, G.J., Brown, C.A., 2009. Scale-based correlations of relative areas with fracture of chocolate, *Wear* 266/5-6, p. 609.
5. Moreno, M.C., Brown, C.A., Bouchon, P., 2010. Effect of food surface roughness on oil uptake by deep-fat fried products, *Journal of Food Engineering* 101, p. 179.
6. Peterson, R.E., 1974. *Stress concentration factors*, John Wiley Sons, New York.
7. Arola D., Ramulu, M., 1999. An examination of the effects from surface texture on the strength of fiber-reinforced plastics. *Journal of Composite Materials* 33, p. 101.
8. Novovic, D., Dewes, R.C., Aspinwall, D.K., Voice, W., Bowen, P., 2004. The effect of machined topography and integrity on fatigue life. *International Journal of Machine Tools & Manufacture* 44.P. 5953.
9. Guillemot N., Lartigue C., Billardon R., Mawussi K., 2010. Prediction of the endurance limit taking account of the microgeometry after finishing milling. *International Journal of Interactive Design and Manufacturing* 4, p. 239.
10. DIN 743-3 Shafts and axles, calculation of load capacity - Part 3: Strength of materials standard published 10/01/2000 by Deutsches Institut Fur Normung E.V. (German National Standard)

11. Quinsat, Y. Sabourin, L. Lartigue, C., 2008, Surface topography in ball end milling process: Description of a 3D surface roughness parameter, *Journal of Materials Processing Technology* 195, 135–143.
12. Quinsat, Y. Sabourin, L. Lartigue, C., 2011 Characterization of 3D surface topography in 5-axis milling, *Wear* 271, 590–595.
13. Denkena, B., BöB, V., Nespor, D., Samp, A., 2011. Kinematic and Stochastic Surface Topography of Machined TiAl6V4-Parts by means of Ball Nose End Milling, 1st CIRP Conference on Surface Integrity 2012, *Procedia Engineering*, Volume 19, 2011, Pages 81-87.
14. Gleason, M. A., Brown, C. A., Moore, J. Z.; Shih, A. J., 2011. "Characterizing Radii on the Tips of Biopsy Needles, .Structured and Freeform Surfaces," Spring Topical Meeting, American Society for Precision Engineering, Raleigh, N.C. ISBN 978-1-887706-57-5.
15. Gleason, M.A., Kordell, S., Lemoine, A., Brown, C.A. , 2013. "Profile Curvatures by Heron's Formula as a Function of Scale and Position on an Edge Rounded by Mass Finishing," 14th International Conference on Metrology and Properties of Engineering Surfaces , Taipei, Taiwan , paper TS4-01, 0022.
16. Guillemot, N., 2010. Prise en compte de l'intégrité de surface pour la prévision de la tenue en fatigue de pièces usinées en fraisage, PhD Thesis, ENS Cachan.
17. Souto-Lebel, A, Guillemot, N, Lartigue, C, Billardon. R. 2011. "Characterization and influence of defect size distribution induced by ball-end finishing milling on fatigue life," 1st CIRP Conference on Surface Integrity 2012, *Procedia Engineering*, 19, 343-348
18. LeGoic G, Brown CA, Favreliere H, Samper S, Formosa F, 2013. Outlier filtering: a new method for improving the quality of surface measurements, *Meas. Sci. Technol.* 24, 015001 (13pp).
19. ISO 25178-2, 2012. Geometrical product specifications (GPS) -- Surface texture: Areal -- Part 2: Terms, definitions and surface texture parameters.
20. ASME B46.1, 2009. Surface Texture: Roughness, Waviness and Lay, American Society of Mechanical Engineers, New York.